Numerical Analysis of Machine Foundation Resting on Saturated Sandy Soil

Dr. Mohammed Y. Fattah
Building and Construction Engineering Department, University of Technology/ Baghdad.
Dr. Nahla M. Salim
Building and Construction Engineering Department, University of Technology/Baghdad.
Wourood T. Al-Shammary
Building and Construction Engineering Department, University of Technology/Baghdad.
Email:wourood.talib@gmail.com

ABSTRACT

The behavior of machine foundation on saturated porous medium can be considered as a complicated geotechnical problem due to nature of dynamic loads and plasticity of soil which make the analysis and design of foundation subjected to dynamic loads more complex. The main criteria for safe performance of machine foundations subjected to dynamic loads are to control excessive displacements. In this paper, a dynamic analysis of strip machine foundation with multiple thicknesses is placed at the middle of the top surface of saturated sand with different states (i.e. loose, medium and dense), and vertical harmonic excitation is carried out and building up of the excess pore water pressure. The dynamic analysis is performed numerically by using finite element software, PLAXIS 2D. The soil is assumed as elastic perfectly plastic material obeys Mohr-Coulomb yield criterion. A parametric study is carried out to evaluate the dependency of machine foundation on various parameters including the amplitude and the frequency of the dynamic load. The dynamic response (displacement and excess pore water pressure) generally increases with increasing of loading amplitude, but the displacement and excess pore water pressure versus frequency are not smooth and exhibit undulations (peaks and troughs).

Keywords: Machine foundation, dynamic loads, finite elements, saturated sand, elastic perfectly plastic.

التحليل العددي لاساس ماكنة على تربة رملية مشبعة

الخلاصة:
ان تصرف اسس المكائن على وسط مسامي مشبع يعتبر مسالة جيوتكنيكية معقدة وذلك يعزى لطبيعة الاحمال الديناميكية ولدونة التربة التي تجعل من عملية التحليل والتصميم للاسس المعرضة للاحمال الديناميكية اكثر تعقيدا. ان المعيار الرئيس لاداء امن لاسس المكائن المعرضة للاحمال الديناميكية هو السيطرة على الازاحات المفرطة. في هذا البحث تم تنفيذ التحليل الديناميكي لاساس ماكنة من نوع شريطي باسماك متعددة وضع بالمنتصف عند السطح العلوي لتربة رملية مشبعة بحالات مختلفة (الرخوة، المتوسطة ، الكثيفة) تحت تاثير الاهتزازات العمودية مع التنبؤ بضغط الماء المتزايد. ان عملية التحليل الديناميكي قد تمت عدديا باستخدام

طريقة العناصر المحددة بواسطة البرنامج ثنائي الابعاد (PLAXIS - 2D). و قد تم تمثيل تصرف التربة بالنموذج المرن- اللدن تماما ويرضخ للمعايير العائدة لـ Mohr-Coulomb. كدراسة حالة قد تم تخمين اعتماديه اسس المكائن على عوامل مختلفة. هذه العوامل: هي القيمة القصوى للحمل الديناميكي و تردد الحمل الديناميكي. و قد وجد أن الاستجابة الديناميكية (الازاحات وضغط الماء المسامي الزائد) عموما تزداد بزيادة القيمة القصوى للحمل الديناميكي ولكن علاقة الازاحات وضغط الماء المسامي الزائد مع التردد لايتبع تصرفا خطيا معتادا بل تموجي (قمم ومنخفضات) وتتفاوت باختلاف الترددات.

INTRODUCTION

Foundations of machines have arbitrary shapes and rigidities and are usually embedded partially in the soil. The supporting soil is of a discrete nature and is a three phase material: solid grains, water and air. Thus soil is not a continuum, nor isotropic or homogeneous and behaves in a complex nonlinear inelastic manner under applied loads. It is well established that the stiffness of the foundations – soil system depends on several factors namely, initial static stress, magnitude of dynamic stress increment, the distribution of stresses over the contact area, variation of shear modulus with depth, layering in the soil medium, embedment of foundation etc.

Dynamic Response of Foundations

Dynamic response of foundations depends on several factors such as the shape, size, flexibility and mass of foundation, the finite depth of stratum over bedrock, the influence of inhomogeneity, anisotropy and nonlinearity of soil and the depth of embedment of the foundation. The following groups of dimensionless parameters which appreciably influence the dynamic response has been identified (Gazetaz, 1983):

1. The ratio H/B of the top layer thickness, H over a critical foundation-plan dimension, B; the latter may be interpreted as the radius, R, of a circular foundation or half the width of a rectangular or a strip foundation.
2. The embedment ratio D/B, where D is the depth from the surface to the horizontal soil-footing interface.
3. The shape of the foundation plan: circular, strip, rectangular, circular ring; in the last two cases the plan geometry may be defamed in terms of the length-to-width or 'aspect ratio', L/B, or the internal-to-external radii ratio, Ri/R , respectively.
4. The frequency factor a_o = ωB/Vs, where Vs is a characteristic shear wave velocity of the soil deposit and ω is the circular frequency.
5. The ratio G_1/G_2 of the shear modulii corresponding to the upper soil layer and the underlying half space, respectively; this ratio may attain values ranging from 0, in case of a uniform stratum on rigid base, to 1, in case of a uniform half space.
6. The Poisson's ratio (s) of the soil layer (s).
7. The hysteretic critical damping ratio (s) ξ of the soil layer (s).

Previous Studies Related to Dynamic Response of Foundation

Spyrakos and Xu (2004) conducted parametric studies to investigate the effects of foundation-soil flexibility and mass as well as foundation embedment on the response. It was concluded that foundation flexibility plays an important role on the dynamic response of foundations, especially for foundations subjected to vertical loads.

First, the effect of foundation flexibility on surface foundations was evaluated. Four relative stiffnesses, K_r and a relative mass density M_r were considered for the

vertical loads. The effect of foundation flexibility on both massless and massive foundations can be evaluated. For both cases, the foundation with the largest and the smallest stiffness correspond to rigid and very soft foundations, respectively, whereas the other two stiffness values correspond to flexible foundations. In order to eliminate the dependence of the results on the shear modulus of the soil and the amplitude of the load, the results were presented in a normalized form and were referred as normalized dynamic compliance.

$$\bar{f} = \frac{G_1 u}{p} = \text{Re}\,[\bar{f}] + \text{Im}\,[\bar{f}] \qquad\qquad .....(1)$$

where: G_1 is the shear modulus of the top soil layer,

   u is the displacement and

   p is the amplitude of the external vertical load.

The dynamic compliance is plotted against the dimensionless frequency $A_o = \omega B/ C_2$ where C_2 is the shear wave velocity of the top soil layer, ω is the frequency of the external load and B is half width of the foundation. For example, the vertical normalized dynamic compliance of a foundation is expressed as: The normalized dynamic compliances at the center of the foundation were plotted versus the nondimensional frequency A_o in Figure (1) for the vertical loads applied at the center. From figure, it was clearly demonstrated that the effects of foundation flexibility are significant. For most of the frequency range studied, the general trend was that the smaller the relative stiffness, the larger the displacement. The ratio of embedment to half width of the foundation is D/B=1.

Three foundations with a relative mass density M_r and relative stiffness values, K_r which could be defined as stiff, soft, and very soft were considered. The normalized dynamic compliances of the foundation subjected to vertical load are plotted in Figure (2) which clearly demonstrates that the effects of foundation flexibility are significant for embedded foundations. Increase of foundation stiffness has a similar effect on the dynamic response of embedded foundations to that of surface foundations. As for surface foundations, comparisons between Figures (1) and (2) show that the relative stiffness plays a greater role on modifying the response of embedded rather than surface foundations. The effects of foundation mass on the response of surface foundations were also investigated. In evaluating the effects of foundation mass, the modulus of elasticity of the foundation was kept constant, while its mass density was varied. The relative foundation stiffness for the vertical load K_r corresponds to intermediate foundation stiffness. From Figure (3), one may observe that by increasing the mass density of the foundation the natural frequency of the system decreases. Foundation mass has a smaller effect on the response compared to that of foundation flexibility. For embedded foundations, the normalized dynamic compliances for vertical loads are drawn in Figure (4).

Baidya and Rathi (2004) investigated the influence of a rigid layer present at different depths, layer of finite thickness underlain by a rigid layer on the dynamic response of a foundation-soil system. Model block vibration tests were carried out in a pit and a vertically acting rotating-mass type mechanical oscillator. Using locally available river sand, a sand layer of six different thicknesses was prepared, and, for each thickness, tests were carried out for two different static weights and three different dynamic loadings as shown in Figure (5). It was concluded that resonant frequency decreased and peak displacement amplitude increased with an increase in thickness of

the layer. Both the resonant frequency and peak displacement amplitude were observed to be almost a constant value when the thickness of the layer exceeded three times the width of footing. The damping ratio of the foundation resting on a finite layer underlain by a rigid layer was obtained from the peak displacement amplitude and was found to be lower compared to the damping of the foundation resting on an infinitely homogeneous soil layer. Further, it was found that the effect of layer thickness on radiation damping is more for a thin layer compared to a thick layer.

Mandal and Roychowdhury (2008) carried out analysis of rectangular raft foundations under transient loading (treated as a free rectangular plate on elastic half-space) by using a coupled finite element –boundary element (FE-BE) approach. The combined stiffness matrix of the plate-half-space was determined by coupling the stiffness matrix of the plate and the half-space matrix obtained from the finite element and boundary element methods, respectively. The half-space response was based on the solution given by Mindlin (1936) for a point load in half-space, which allows taking into account the effect of embedment of the plate. The governing differential equation for the raft-soil system subjected to transient loading was solved by using Newmark integration method. Parametric study on response was carried out. It was noted that the increase in damping of the system reduces the amplitude of response but its effect on frequency of response is not significant. It was observed that increase in the thickness of the raft reduces the amplitude as well as the frequency of response considerably. The effect of shape (aspect ratio) on the response of rectangular rafts was studied. It was noted that the amplitude of response is lowest for the square raft (aspect ratio = 1.0), the frequency of response was not significantly affected by the aspect ratio.

Ramesh et al. (2008) studied the influence of rigid boundary underlying sand bed on vertical vibrations of massless rigid footings experimentally by subjecting them to vertical vibrations and it was concluded that presence of rigid base at shallow depth significantly influences the resonant frequency of soil foundation system. Mass of foundation resting over rigid base has an influence on the vertical mode of vibration. As the thickness of sand bed increases, the resonant frequency increases which is probably due to wave attenuation and reflection due to the presence of rigid boundary at shallow depth and the footing blocks are having very less mass. Also, it was observed that the value of damping ratio increases with increase in size of footing and thickness of sand bed and does not vary with eccentricity and the stiffness of the soil increases with increase in mass of footing.

Ramesh and Kumar (2011) made a parametric study on the influence of the rigid base on the response of the foundation-soil system. Two types of extremities, such as, the presence of uniform stratum over a rigid base and on top of a half-space have been simulated by compacting sand beds to different depths over a finite stratum represented by the rigid concrete base and the more flexible natural red earth base. The results were compared for both cases. Two series of reinforced model footings of square shape and of different thicknesses were cast and cured. It was found that the resonant frequency decreases significantly with increase in H/B ratio between 0.5 to 2.0, corresponding to the cases viz., rigid concrete base and the natural red-earth base. Higher the contact area, greater is the resonant frequency and for a constant area of the footing-larger the mass (increase in thickness), lower is the resonant frequency, for both the types of finite base. With increase in the mass ratio, the resonant frequency decreases and this decrease is more significant with increase in H/B ratio

between 0.5 and 1.0. Lower the mass ratio, higher will be the resonant frequency under a given H/B ratio of sand.

Fattah et al. (2013) used the finite element method in an attempted to study liquefaction of soil based on the case solved previously by transient infinite element for 2D soil - structure interaction analysis considering infinite boundaries but without generation of pore water pressure. The properties of fully saturated sandy soil and concrete are fed to geotechnical finite element software called QUAKE/W program. The results showed that liquefaction occurs faster at shallow depths due to low overburden pressure. Also, liquefaction zones and deformation occur faster with the increase of dynamic loading amplitude. The analysis marked that increasing the amplitude pressure accelerates the occurrence of initial liquefaction and increases the pore water pressure. Tracing the propagation of liquefaction zones, one can notice that liquefaction occurs first near the loading end and then develops faraway.

Definition of the Basic Problem

Dynamic finite element analysis of strip foundation under vertical harmonic excitation is carried out in this paper. A 3 m wide strip foundation with multiple thicknesses is placed at the middle of the top surface of sand with different states (i.e. loose, medium and dense). The analysis is performed numerically using the finite element software, PLAXIS 2D version 8.2. 15-noded triangular isoparametric elements are used to discretize the soil medium under the plane strain condition. The boundaries of the soil are taken as (30 m) wide and (20 m) deep far away from the foundation to minimize the boundary effect. To investigate the excess pore water pressure build up under machine foundation due to harmonic excitation, the soil is assumed to be saturated with water table coincides with the ground surface. The boundary conditions and other modeling details considered for strip foundation are shown in Figure (6). Total fixities ($u_x = u_y = 0$) are applied at the base of the model

and horizontal fixities ($u_x = 0$) are applied at the extreme vertical boundaries restraining the motion along the horizontal direction. Absorbent boundaries are applied along vertical and horizontal boundaries to avoid the reflection of stress waves back to the failure domain.

It should be noted that in this analysis, a vertical vibration is applied and the vertical displacements and excess pore water pressure are measured at the top central point of the foundation (node A in Figure 6). It is important to mention here that all cases are analyzed for duration of (60 sec) with time step taken as ($\Delta t = 0.0256$ sec).
The computer program PLAXIS is used for numerical modeling of the problem; this program has a series of advantages. It has the ability to deal with excess pore-pressure phenomena. Excess pore pressures are computed during plastic calculations in undrained soil (Catala, 2005).

Material Properties

The properties are classified into two groups:
1.   **Soil properties**: Three states of sandy soil are used in this parametric study which are: loose, medium and dense sand. The soil deposit is assumed to obey the advanced Mohr-Coulomb yield criterion, with parameters adopted from Bowles (1996) and Murthy (2006) except the dilatancy parameter. The effect of dilatancy is taken into account in the present study. The dilatancy of sand depends on both the density and the friction angle. It is suitable in PLAXIS to use the value of cohesion c

> 0.2 kPa for cohesionless sands and dilatancy angle $\psi = \emptyset - 30$ for the soils with $\emptyset >$ 30, and $\psi = 0$ for the soils with $\emptyset < 30$ [7]. Due to this, the value of cohesion is assumed equal to 1 kPa to avoid complications and the value of the angle of dilatancy is assumed as ($\psi = \emptyset - 30$). The properties of all soil types are listed in Table (1).

2. **Foundation properties**: The concrete foundation is assumed as a linear elastic material with parameters shown in Table (1). The weight of the machine depends upon its type as suggested by Leonards (1962). Based on this table, the ratio between weight of foundation and weight of machine is approximately taken as 2.16 (i.e. weight of machine = 10 kN).

Sinusoidal excitation
The most common problem involving dynamic loading is that of foundation for machinery. Reciprocating machines and poorly balanced rotating equipment cause periodic dynamic forces $f(t)$ (Li and Borja, 2005):

$$f(t) = a \sin \omega t \qquad \qquad .....(2)$$

where:

a = maximum amplitude of dynamic force,

$\omega = 2\pi f$ with f = operating frequency,

t = time.

Typical operating frequencies range from (3 Hz) for large reciprocating air compressors to about (200 Hz) for turbines and high-speed rotary compressors (Al-Sherefi, 2000). The values of amplitudes range between 25 and 100 kPa while the frequency range between 5 and 50 Hz.

Effect of Harmonic Loading Parameters
Loading and consequently the amount of displacement has a significant effect on the accuracy of analyses (effect of strain range) and determining the range of displacement in which accurate results can be obtained from each model is an important issue. Therefore, effect of external loading on the model has been studied in two different manners. First, all parameters of the model are kept constant and only the amount of loading frequency is varied. In the second manner, all parameters of the model are kept constant and only the amount of amplitude of loading is increased.

Effect of loading frequency
A sinusoidal wave loading is applied on the top of foundation for a period of (60 sec) with constant amplitude while the frequency is changed (5, 25, 35 and 50 Hz). The corresponding displacements are monitored at node (A) at center of the foundation. Figures (7), (9), (11) and (13) demonstrate the typical displacement-time relations for loose, medium and dense sand, while Figures (8), (10), (12) and (14) show the typical excess pore water pressure-time relations for loose, medium and dense sand with the same amplitude of sinusoidal loading, thickness of foundation and values of loading frequencies.
For loose sand, it can be seen that the magnitude of displacement at the base of the foundation is found to increase gradually with time with almost identical value at earlier stages at (20 sec), after that these values reach a steady state as the time progresses. It can also be noticed that the displacement becomes in the negative zone of the displacement-time response, the shapes of the displacement versus time for

loose sand generally follow this trend, due to the plastic behavior of Mohr-Coulomb analysis. This observation agrees well with Mandal and Roychowdhury (2008). When the frequency range is between (5-25 Hz), the vertical displacement decreases at node (A) by (84%), while for frequency between (25-35 Hz), it increases by (386%), but the displacement at frequency range (35-50 Hz) returns to decreases by about (32%).

On the other hand, the time histories of the excess pore water pressure at node (A) located at the surface along the center line of the foundation, the excess pore water pressure is defined as the incremental pore water pressure generated by the application of machine loading on top of the foundation. It can be noted that as time progresses, the results tend to increase in extension positive zone of the excess pore water pressure -time response. This trend is due to the buildup of excess pore water pressure within the soil. These results are consistent in trend with the numerical and experimental studies of (A-Sherefi, 2000); Li and Borja (2005); Al-Wakel (2010). It can also be noticed that the increase in the frequency from (5 to 25 Hz) leads to increase in excess pore water pressure by about (33%), while for frequency between (25-35 Hz), the pore water pressure decreases by (27%) but for frequency range (35-50 Hz) the excess pore water pressure returns to increase by about (25%).

For medium sand, the figures show that when the frequency range is between (5-25 Hz), the vertical displacement decreases at point (A) by (83%), while for frequency between (25-35 Hz) the vertical displacement increases by (400%), but it returns to decrease by (33%) at frequency range (35-50 Hz).

On the other hand, the increase in the frequency from (5 to 25 Hz), leads to increase in the excess pore water pressure at point (A) by about (35%). Further increase in the frequency between (25-35 Hz) causes decrease in the excess pore water pressure by (22%) due to cyclic mobility (when the sand sample has undergoes initial liquefaction accompanied by the well-known cyclic mobility phenomenon based on the effective stress principle [11], while for frequency between (25-35 Hz), the excess pore water pressure increases by (16%). It can also be noted that the maximum excess pore water pressure takes place at frequency (25 Hz).

For dense sand, the figures reveal that the vertical displacement decreases when the frequency range is between (5-25 Hz) by (71%) at point (A), while for frequency range (25-35 Hz), the vertical displacement increases by (336%), but the displacement at frequency range (35-50 Hz) returns to decrease by (51%). It is worth mentioning that the portion of the typical response curve will be in positive zone of the displacement-time response. This leads to the conclusion that, increasing the modulus of elasticity reduces plastic strain and makes the behavior closer for elastic behavior and the elastic-plastic behavior of soil would be negligible in dense sand. Plastic behavior of Mohr-Coulomb analysis would be negligible in dense sand as stated by Mandal and Roychowdhury (2008). On the other hand, the cumulative excess pore water pressure develops from the start of harmonic loading. It can be noticed that when the frequency of harmonic loading increases from (5 to 25 Hz), the excess pore water pressure at point (A) increases by about (34%), while for frequency between (25-35 Hz) decreases by (19%) due to cyclic mobility, but at frequency range (35-50 Hz) returns to decrease by (7 %).

Effect of loading amplitude

   Two values of loading amplitude (a=50 and 100 kN/m^2) where (amplitude a = 25 kN/m^2 is investigated in the previous section) are used without damping and load frequency equal (5 Hz).

Figures (15) and (17) manifest the typical displacement-time responses for loose, medium and dense sand at different values of load amplitude (a = 50, and 100 kN/m^2), while Figures (16) and (18) show the typical excess pore water pressure-time responses for loose, medium and dense sand with same frequency of sinusoidal loading, thickness of foundation and values of loading amplitude.

   For loose sand, it can be noticed that by duplicating the amplitude of loading from (50 to 100 kN/m^2), the displacement at point (A) increases by about (130%). This is compatible with the finding of Jesmani and Kamalzare (2010) who found that by increasing the magnitude of loading and consequently increasing the plastic and elastic strain with nonlinear fashion, the behavior of soil becomes non-linear.

On the other hand, the cumulative pore pressure develops from the start of sinusoidal loading. The pore water pressure is positive at the wave crest and negative at the wave trough. It can be seen that when the sinusoidal loading amplitude was changed from (50 kN/m^2) to (100 kN/m^2), a sudden pore water pressure increase by about (67%) takes place at first and with a continued accumulation thereafter. This conclusion agrees well with Yang et al. (2003) who stated that the amplitude of cyclic load has a considerable influence on the generated pore water pressure. The amplitude of pore water pressure decreases gradually during cyclic loading for loose sand, but the average value increases faster and faster. This behavior is accompanied by large deformations.For medium sand, by doubling the amplitude of sinusoidal loading from (50 to 100 kN/m^2), the vertical displacement intensifies by (150%). From figures which show the time histories of the excess pore water pressure at node (A), located directly below the center of the foundation, the excess pore water pressure increases by about (60%).   For dense sand, from the typical displacement-time response, it can be concluded that the vertical displacement increases by (140%) by doubling the amplitude of sinusoidal loading from (50 to 100 kN/m^2).

 On the other hand, the magnitude of excess pore water pressure increases by about (50%). Dense sand has a dilative behavior at high strain levels, and the corresponding shear stresses may be extremely low Yang et al. (2003).

Resonant frequency

   All machines under operation usually induce a periodic dynamic load on the foundation. Due to this induced dynamic load from the machine, the foundation including some portion of the soil underlying the foundation is subjected to vibration and it's essential that the natural frequency (ω_n) of this vibration should be well away from the operating frequency of the machine (Chowdhury and Dasgupta, 2010), (ω_n) of the system is expressed as (Rao, 2011):

$$\omega_n = \sqrt{\frac{k}{m}} \qquad\qquad ..... (3)$$

where:

   k = equivalent spring constant, and

  m = mass of machine and foundation.

If the effect of the soil (m_s) is taken into account, the expression as shown in Equation (3) becomes (Rao, 2011):

$$\omega_n = \sqrt{\frac{k}{m+m_s}} \quad \text{and} \quad f_n = \frac{1}{2\pi}\sqrt{\frac{k}{m+m_s}} \qquad \text{..... (4)}$$

where:

  m = total mass of foundation and machine (kg), m = $\frac{w}{g}$,

  w = weight of foundation (kN), w = L $\times$ B $\times$ h $\times$ $\gamma_{concrete}$ = length, width, thickness of foundation (m) and unit weight of the concrete foundation (kN/m^3) respectively,

  g = acceleration due to gravity (m/sec^2),

  f_n = natural frequency in (Hz), and

  m_s = mass of soil participating in vibration (kg).

There have been several approaches suggested to determine the effective or equivalent mass of soil (m_s), in calculating the natural frequency (Rao, 2011). The choice of any one method still remains the designer's preference. Catala (2005) suggested that the mass of the vibrating soil should lie between (2/3) to (1.5) times the total mass of the vibrator and foundations; therefore the mass of soil is considered to be equal to the total mass of the vibrator and foundations in this study.

  The equivalent spring constant can be calculated from the Lysmer and Richart's method (1970) (Richat et al., 1970):

$$K = \frac{4G\,r_0}{1-v} \qquad \text{..... (5)}$$

where:

  G = shear modulus of the soil (kN/m²), $G = \frac{E}{2(1+v)}$

  E = Young's modulus of soil (kN/m²),

  v = Poisson's ratio of soil, and

  r_0 = equivalent radius of the foundation (m) $=\left(\frac{L\,B}{\pi}\right)^2$.

Accordingly, the frequency ratio is defined as the ratio of operating frequency (*f*) to natural frequency (f_n). The frequency ratio ($\frac{f}{f_n}$) should be either less than 0.5 or more than 2 to avoid resonance (Rao, 2011). The values of the natural frequency (f_n) and frequency ratio ($\frac{f}{f_n}$) are summarized in Table (2).

The relations obtained from different load amplitudes and frequencies

  Figure (19) depicts the relationships between the frequency ratio (*f*/f_n) and the maximum vertical displacement for three amplitudes of vertical harmonic load for machine foundation constructed over loose, medium and dense sand. It can be noticed that, the relationships are not smooth but exhibit undulations (peaks and troughs) associated with the natural frequencies (in shear and dilation) of the soil layer. The

maximum displacement for three amplitudes applied was found to be at frequency ratio of (0.344), (0.24) and (1.217) for loose, medium and dense sand, respectively. These findings maintain that the frequency ratio is either less than 0.5 or more than 2 for machines to avoid resonance condition except in the case of dense sand. It is noticeable that by decreasing amplitude of vibration, the flatness of the curve increases and the peak value of the relation become little. It is worth noting that, the curves for the three amplitudes coincide with almost identical value at frequency ratio equal to the (1.721) for loose sand, and (1.202) for medium sand.

From Figure (20) which presents the relationships between the frequency ratio (f/f_n) and the maximum excess pore water pressure for three amplitudes of vertical harmonic load for machine foundation constructed over loose, medium and dense sand, it can be seen that the maximum excess pore water pressure follows the simultaneous behavior for the deformation, these observations qualitatively agree with previous findings in trend of Yang et al., (2003). The peak of excess pore water pressure increases as the amplitude of the vibration increases and it is focused at frequency ratios (1.721), (1.202), (0.87) for loose, medium and dense sand, respectively.

Figure (21) shows the relationships between the amplitude of machine loading and the maximum vertical displacement for four frequencies of vertical harmonic load for machine foundation constructed over loose, medium and dense sand. It can be indicated that the maximum vertical displacement increases linearly as the amplitude of the machine loading increases. The maximum vertical displacement occurred at frequency (5 Hz), (5 Hz) and (35 Hz) for loose, medium and dense sand, respectively.

Figure (22) presents the relationships between the amplitude of machine loading and maximum excess pore water pressure for four frequencies of vertical harmonic load for machine foundation constructed over loose, medium and dense sand. It can be seen that the maximum excess pore water pressure takes place at frequency (25 Hz) for all soil types. These conclusions qualitatively agree with those reported by in trend (Chang et al., 2007).
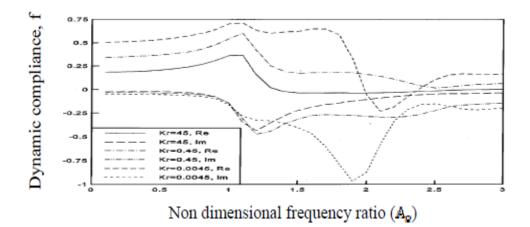

Figure (1) - Effect of foundation stiffness for surface foundation subjected to vertical loads (after Spyrakos and Xu, 2004).
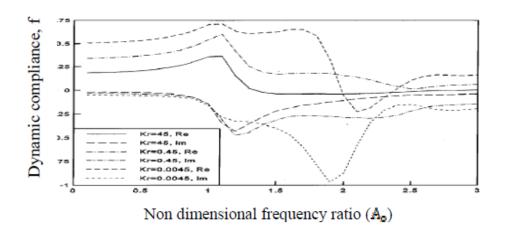
Figure (2) - Effect of foundation stiffness for embedded foundation subjected to vertical loads (after Spyrakos and Xu, 2004).

Figure (3) - Effect of foundation mass for surface foundation subjected to vertical loads (after Spyrakos and Xu, 2004).
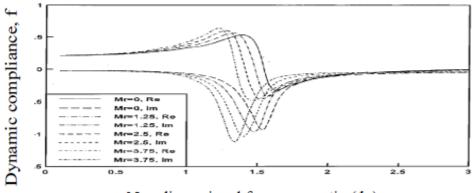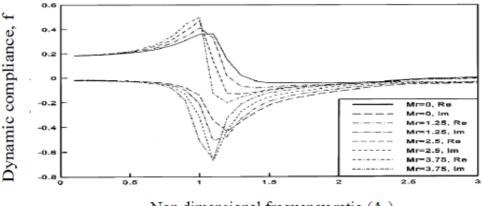

Figure (4) - Effect of foundation mass for embedded foundation subjected to vertical loads (after Spyrakos and Xu, 2004).
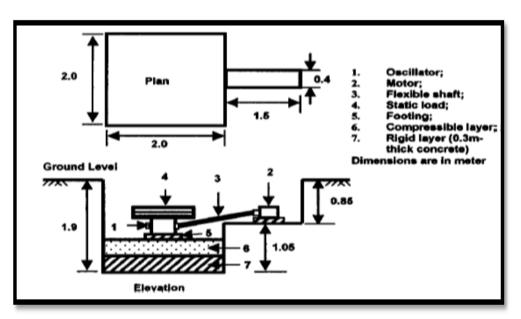
**Figure .(5) - Schematic diagram of the pit geometry and experimental setup
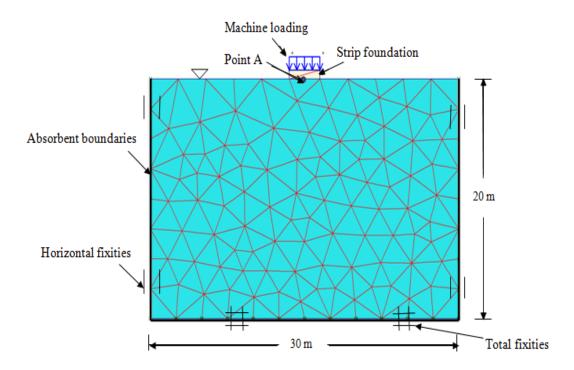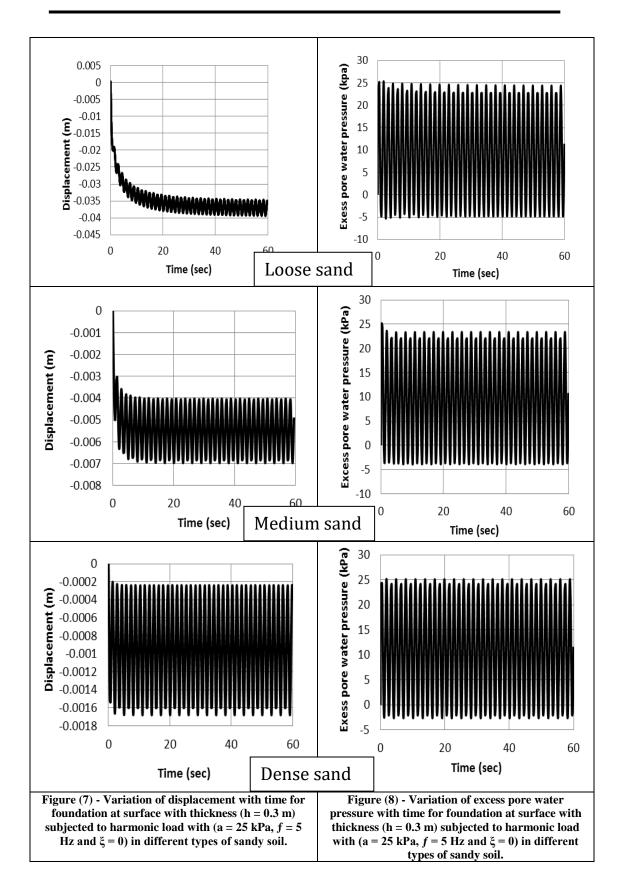(Baidya and Rathi, 2004).**

**Figure (6) Finite element mesh and boundary condition of the machine
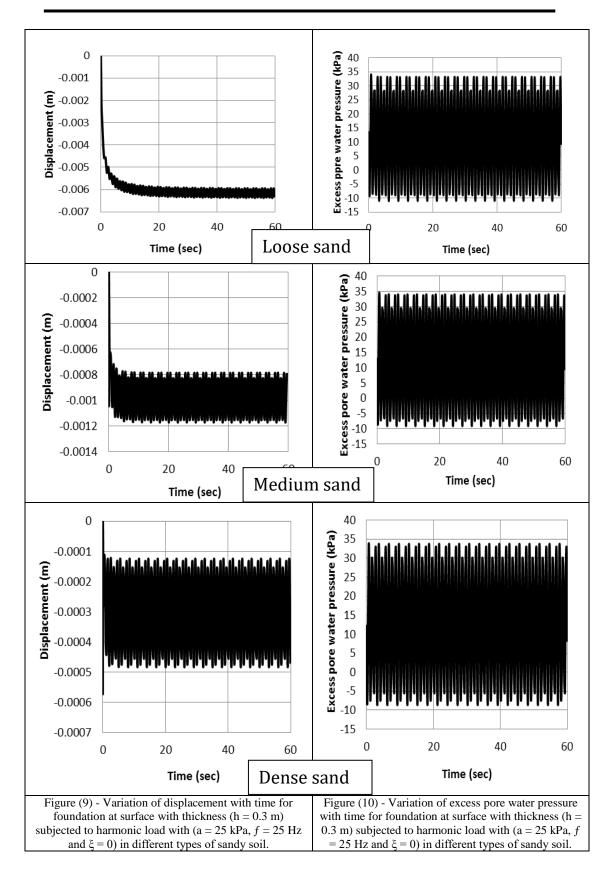foundation problem.**

Table (1) - Material properties.

Material	Material properties	Unit	Loose sand	Medium sand	Dense sand
Soil	Unit weight, γ	(kN/m³)	16	18.5	21
	Young's modulus, E	(kN/m²)	18000	35000	65000
	Poisson's ratio, ν	-	0.3	0.32	0.34
	Friction angle, □	(°)	32	35	40
	Cohesion, c	(kN/m²)	1	1	1
	Dilatancy angle, ψ	(°)	2	5	10
	Horizontal permeability, k_x	(m /sec)	10^{-3}	10^{-4}**	10^{-5}**
	Vertical permeability, k_y	(m /sec)	10^{-3}	10^{-4}***	10^{-5}**
Foundation	Young's modulus of concrete, $E_{concrete}$	(kN/m²)	2×10^7*		
	Unit weight of concrete, $\gamma_{concrete}$	(kN/m³)	24*		
	Poisson's ratio of concrete, $\nu_{concrete}$	-	0.15**		
Machine	Weight of machine, $W_{mach.}$	(kN)	10 *		

Table (2) - Frequency ratios for all soil types and thicknesses of foundation.

Type of soil	G (kN/m²)	K (kN/m)	h (m)	m + m_s (Kg)	f_n (Hz)	f (Hz)	$\dfrac{f}{f_n}$
Loose sand	6923.07	36637.5	0.3	4.4	14.523	5	0.344
						25	1.721
						35	2.41
						50	3.442
			0.5	7.3	11.275	5	0.443
						25	2.217
						35	3.104
						50	4.435
			0.75	11	9.185	5	0.544
						25	2.722
						35	3.811
						50	5.443
Medium sand	13257.575	75153.844	0.3	4.4	20.8	5	0.24
						25	1.202
						35	1.682
						50	2.403
			0.5	7.3	16.149	5	0.31
						25	1.548
						35	2.167
						50	3.1
			0.75	11	13.155	5	0.38
						25	1.9
						35	0.376
						50	3.8
Dense sand	24253.731	143611.488	0.3	4.4	28.753	5	0.174
						25	0.87
						35	1.217
						50	1.74
			0.5	7.3	22.323	5	0.224
						25	1.12
						35	1.568
						50	2.24
			0.75	11	18.185	5	0.275
						25	1.375
						35	1.925
						50	2.75

Loose sand

Medium sand

Dense sand

Figure (7) - Variation of displacement with time for foundation at surface with thickness (h = 0.3 m) subjected to harmonic load with (a = 25 kPa, ƒ = 5 Hz and ξ = 0) in different types of sandy soil.	**Figure (8) - Variation of excess pore water pressure with time for foundation at surface with thickness (h = 0.3 m) subjected to harmonic load with (a = 25 kPa, ƒ = 5 Hz and ξ = 0) in different types of sandy soil.**

Loose sand

Medium sand

Dense sand

Figure (9) - Variation of displacement with time for foundation at surface with thickness (h = 0.3 m) subjected to harmonic load with (a = 25 kPa, ƒ = 25 Hz and ξ = 0) in different types of sandy soil.	Figure (10) - Variation of excess pore water pressure with time for foundation at surface with thickness (h = 0.3 m) subjected to harmonic load with (a = 25 kPa, ƒ = 25 Hz and ξ = 0) in different types of sandy soil.

Loose sand

Medium sand

Dense sand

| Figure (11) - Variation of displacement with time for foundation at surface with thickness (h = 0.3 m) subjected to harmonic load with (a = 25 kPa, *f*=35 Hz and ξ = 0) in different types of sandy soil. | Figure (12) - Variation of excess pore water pressure with time for foundation at surface with thickness (h = 0.3 m) subjected to harmonic load with (a = 25 kPa, *f* = 35 Hz and ξ = 0) in different types of sandy soil. |

Loose sand

Medium sand

Dense sand

Figure (13) - Variation of displacement with time for foundation at surface with thickness (h = 0.3 m) subjected to harmonic load with (a = 25 kPa, ƒ = 50 Hz and ξ = 0) in different types of sandy soil.	Figure (14) - Variation of excess pore water pressure with time for foundation at surface with thickness (h = 0.3 m) subjected to harmonic load with (a = 25 kPa, ƒ = 50 Hz and ξ = 0) in different types of sandy soil.

Loose sand

Medium sand

Dense sand

Figure (15) - Variation of displacement with time for foundation at surface with thickness (h = 0.3 m) subjected to harmonic load with (a = 50 kPa, ƒ=5 Hz and ξ = 0) in different types of sandy soil.	Figure (16) - Variation of excess pore water pressure with time for foundation at surface with thickness (h = 0.3 m) subjected to harmonic load with (a = 50 kPa, ƒ = 5 Hz and ξ = 0) in different types of sandy soil.

Loose sand

Medium sand

Dense sand

Figure (17) - Variation of displacement with time for foundation at surface with thickness (h = 0.3 m) subjected to harmonic load with (a = 100 kPa, *f* = 5 Hz and ξ = 0) in different types of sandy soil.	Figure (18) - Variation of excess pore water pressure with time for foundation at surface with thickness (h = 0.3 m) subjected to harmonic load with (a = 100 kPa, *f* = 5 Hz and ξ = 0) in different types of sandy soil.

a.   Loose sand.

b.   Medium sand.

c.   Dense sand.

Figure (19) - Variation of the maximum displacement with frequency ratio for foundation at surface with thickness (h = 0.3 m) and without damping (ξ = 0) for loose, medium and dense sandy soil.

a.   Loose sand.

b.   Medium sand.

c.   Dense sand.

Figure (20) - Variation of the maximum excess pore water pressure with frequency ratio for foundation at surface with thickness (h = 0.3 m) and without damping (ξ = 0) for loose, medium and dense sandy soil.

a.   Loose sand.

b.   Medium sand.

c.   Dense sand.

Figure (21) - Variation of the maximum displacement with amplitude for foundation at surface with thickness (h = 0.3 m) and without damping (ξ = 0) for loose, medium and dense sandy soil.

a.   Loose sand.

b.   Medium sand.

c.   Dense sand.

Figure (22) - Variation of the maximum excess pore water pressure with amplitude for foundation at surface with thickness (h = 0.3 m) and without damping ($\xi = 0$) in loose, medium and dense sandy soil.

CONCLUSIONS

From the extended parametric study carried out in this paper by utilizing the finite element program PLAXIS 2D V8.2 for analysis of machine foundation rested on sandy soil with different densities, the following conclusions can be drawn:

2-   For foundation at surface resting on sand of different relative densities, relations between frequency with displacement and excess pore water pressure are not smooth and exhibit undulations (peaks and troughs), but for all cases, the maximum displacement occurs at frequency 5 Hz and maximum pore water pressure occurs at frequency 25 Hz.

3-   For foundation at surface and embedded foundation resting on sand of different relative densities, the displacement and excess pore water pressure increase approximately in a linear fashion with increasing amplitude of dynamic loading.

4-   The maximum excess pore water pressure follows the simultaneous behavior for the deformation.

5-   The maximum vertical displacement increases linearly as the amplitude of the machine loading increases. The maximum vertical displacement occurred at frequency (5 Hz), (5 Hz) and (35 Hz) for loose, medium and dense sand, respectively. The maximum excess pore water pressure takes place at frequency (25 Hz) for all soil types.

REFERENCES

[1]Al-Sherefi, M. H. J. (2000): "Non-Linear Dynamic Response of Soils," MSc. Thesis, University of Baghdad.

[2]Al-Wakel, S. F. (2010): "Experimental and Numerical Investigations of Foundation Vibrations", Ph.D. Thesis, Building and Construction Engineering Department, University of Technology, Baghdad, Iraq.

[3] Baidya, D. K., and Rathi, A. (2004): "Dynamic Response of Footing Resting on a Sand Layer of Finite Thickness", Journal of Geotechnical and Geoenvironmental Engineering, ASCE, Vol. 130, No. 6, pp. 651-655.

[4] Bowles, J. E. (1996) "Foundation Analysis and Design", 5th edition McGraw-Hill Companies, Inc., pp. 1175.

[5] Brinkgreve, R. B, J. (2002): "PLAXIS-2D Version 8 User Manuals", Delft University of Technology and PLAXIS, b. v., the Netherlands.

[6]Catala , M. A. (2005): "Excess Pore Pressure Generation due to Pseudostatic Tests in Saturated Sand", Ph.D. Thesis, Delft University of Technology, Netherland.

[7] Chang, W. J., Rathje, E. M., Stokoe, K. H. and Hazirbaba, K. (2007): "In Situ Pore-Pressure Generation Behavior of Liquefiable Sand", Journal of Geotechnical and Geoenvironmental Engineering, ACSE, Vol. 133, No. 8, pp. 921-931.

[8] Chowdhury, I., and Dasgupta, S. P. (2009): "Dynamics of Structures and Foundations – A unified Approach", CRC Press-Balkema, London.

[9] Das. B.M. and Ramana, G. V. (2010), "Principles of Soil Dynamics", Cengage Learning, Inc second edition.

[10]Fattah, M. Y., Mohammed A. Al-Neami., and Nora Hameed Jajjawi. (2013): "Implementation of Finite Element Method for Prediction of Soil Liquefaction Around Undergroud Structure", Journal of Engineering and Technology, University of Technology., Vol. 31, No. 4, pp. 703-714.

[11] Gazetas, G. (1983): "Analysis of Machine Foundations: State of the Art", Soil Dynamics and Earthquake Engineering, Vol. 2, No. 1, pp. 2-42.

[12] Jesmani, M., and Kamalzare, M. (2010): "Comparison between Numerical and Analytical Solution of Dynamic Response of Circular Shallow Footing", Electronic Journal of Geotechnical Engineering, EJGE, Vol. 15, Bund. p, pp. 1768-1780.

[13] Lambe, T. W. and Whitman, R. V. (1979): "Soil Mechanics," John Wiley and Sons.

[14] Leonards, G.A. (1962): "Foundation Engineering", McGraw-Hill Book Co., Inc., New York, USA.

[15]Li, C. and Borja, R.J. (2005), "Finite Element Formulation of Poro-Elasticity Suitable for Large Deformation Dynamic analysis", Report No.147, Department of Civil and Environmental Engineering, University of Stanford.

[16] Mandal, J. J., and Roychowdhury, S. (2008): "Response of Rectangular Raft Foundations under Transient Loading", Proceedings, 12th International Conference of International Association for Computer Methods and Advanced in Geomechanis (IACMAG), India, pp. 524-530.

[17]Mindlin, R. D. (1936): "Force at a Point in the Interior of a Semi-Infinite Solid", Physics, pp. 227-235 (Cited by Mandal, and Roychowdhury, 2008).

[18] Murthy, V. N. S. (2006): "Geotechnical Engineering, Principles and Practices of Soil Mechanics and Foundation Engineering", Marcel Dekker, Inc. New York.

[19]Ramesh, H. N., Raghavendra Rao, M. V., Kumar. M. T., and Bhavya, M. (2008): "Dynamic Response of Model Footing over a Rigid Base under Vertical Vibration", Proceedings, 12th International Conference of International Association for Computer Methods and Advanced in Geomechanis (IACMAG), India, pp. 2680-2687.

[20] Ramesh, H. N., and Kumar. M. T. (2011): "Concepts and Problems in the Design of Foundations Subjected to Vibrations", International Journal of Geomechanics, ASCE, pp. 312-321.

[21]Rao, N. S. V. (2011), "Foundation Design: Theory and Practice", John Wiley & Sons (Asia),

[22] Richart, F. E., Hall, J. R., and Woods, R. D. (1970): "Vibrations of Soils and Foundations", Prentice-Hall, Englewood Cliffs, N.J., 414 pp.

[23] Spyrakos C.C., and Xu C. (2004): "Dynamic Analysis of Flexible Massive Strip Foundations Embedded in Layered Soil by Hybrid BEM-FEM", Soil Dynamics and Earthquake Engineering, Vol. 82, pp. 2541-2550.

[24] Yang, S., Sandven, R. and Grande, L. (2003): "Liquefaction of Sand under Low Confining Pressure", Journal of Ocean University of Qingdao, Vol. 2, No. 2, pp. 207-210.